ADVANCED MATERIALS

Supporting Information

for *Adv. Mater.,* DOI: 10.1002/adma.202207436

High Entropy Approach to Engineer Strongly Correlated Functionalities in Manganites

Abhishek Sarkar, Di Wang,* Mohana V. Kante, Luis Eiselt, Vanessa Trouillet, Gleb Iankevich, Zhibo Zhao, Subramshu S. Bhattacharya, Horst Hahn, and Robert Kruk**

High entropy approach to engineer strongly-correlated functionalities in manganites

Abhishek Sarkar[a,b,*], *Di Wang*[b,c,*], *Mohana V. Kante*[b], *Luis Eiselt*[a], *Vanessa Trouillet*[c,d], *Gleb Iankevich*[b,e], *Zhibo Zhao*[b], *Subramshu S. Bhattacharya*[f], *Horst Hahn*[a,b,e] *and Robert Kruk*[b,*]

[a]KIT-TUD Joint Research Laboratory Nanomaterials – Technische Universität Darmstadt, *Otto-Berndt-Str. 3,* 64287 Darmstadt, Germany

[b]Institute of Nanotechnology, Karlsruhe Institute of Technology, Hermann-von-Helmholtz-Platz 1, 76344 Eggenstein-Leopoldshafen, Germany

[c]Karlsruhe Nano Micro Facility (KNMFi), Karlsruhe Institute of Technology (KIT), Hermann-von-Helmholtz-Platz 1, 76344 Eggenstein- Leopoldshafen, Germany

[d]Institute for Applied Materials (IAM-ESS), Karlsruhe Institute of Technology (KIT), Hermann-von-Helmholtz-Platz 1, 76344 Eggenstein- Leopoldshafen, Germany

[e]Institute for Quantum Materials and Technologies (IQMT), Karlsruhe Institute of Technology, Hermann-von-Helmholtz-Platz 1, 76344, Eggenstein-Leopoldshafen, Germany

[f]Nanofunctional Materials Technology Centre (NFMTC), Department of Metallurgical and Materials Engineering, Indian Institute of Technology Madras, Chennai-600036, India

*Corresponding authors: abhishek.sarkar@kit.edu, di.wang@kit.edu, robert.kruk@kit.edu

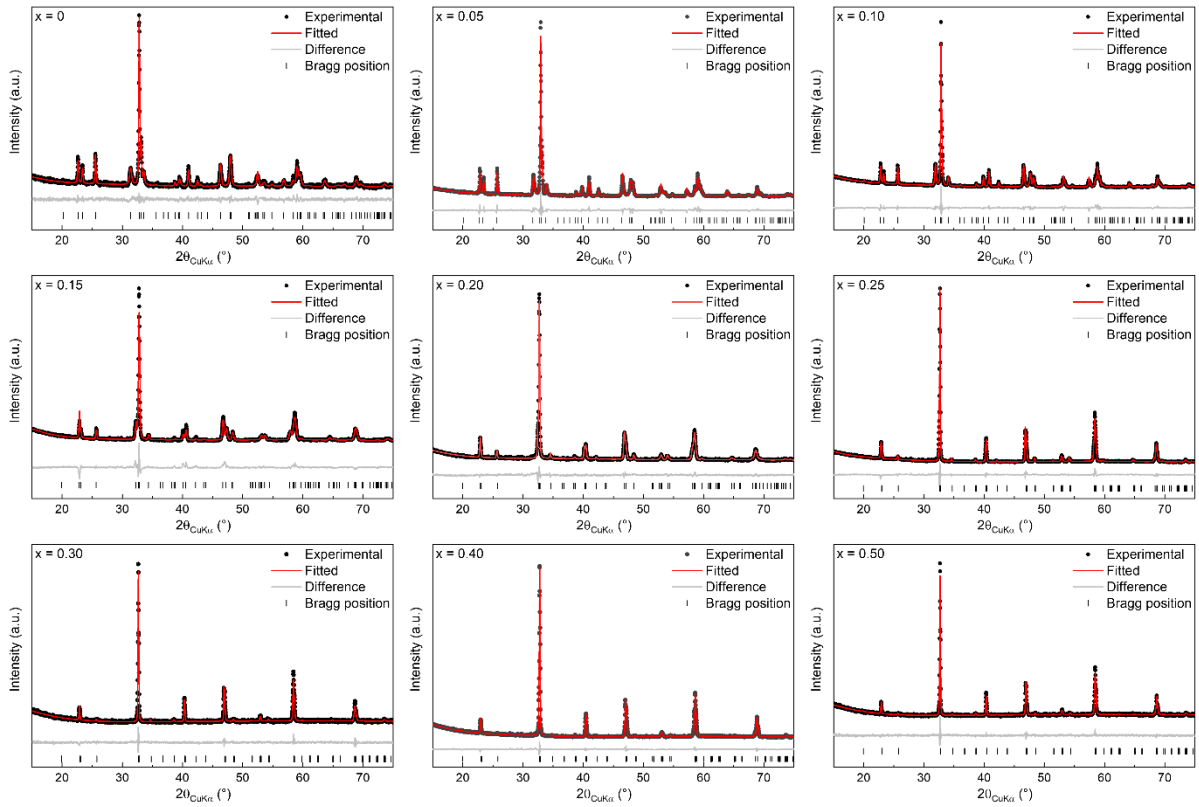

Figure S1. Rietveld refinement of XRD patterns showing single phase orthorhombic structure for all the compositions. Anisotropic strain broadening using was used to adequately fit the XRD pattern for x = 0 and 0.05.

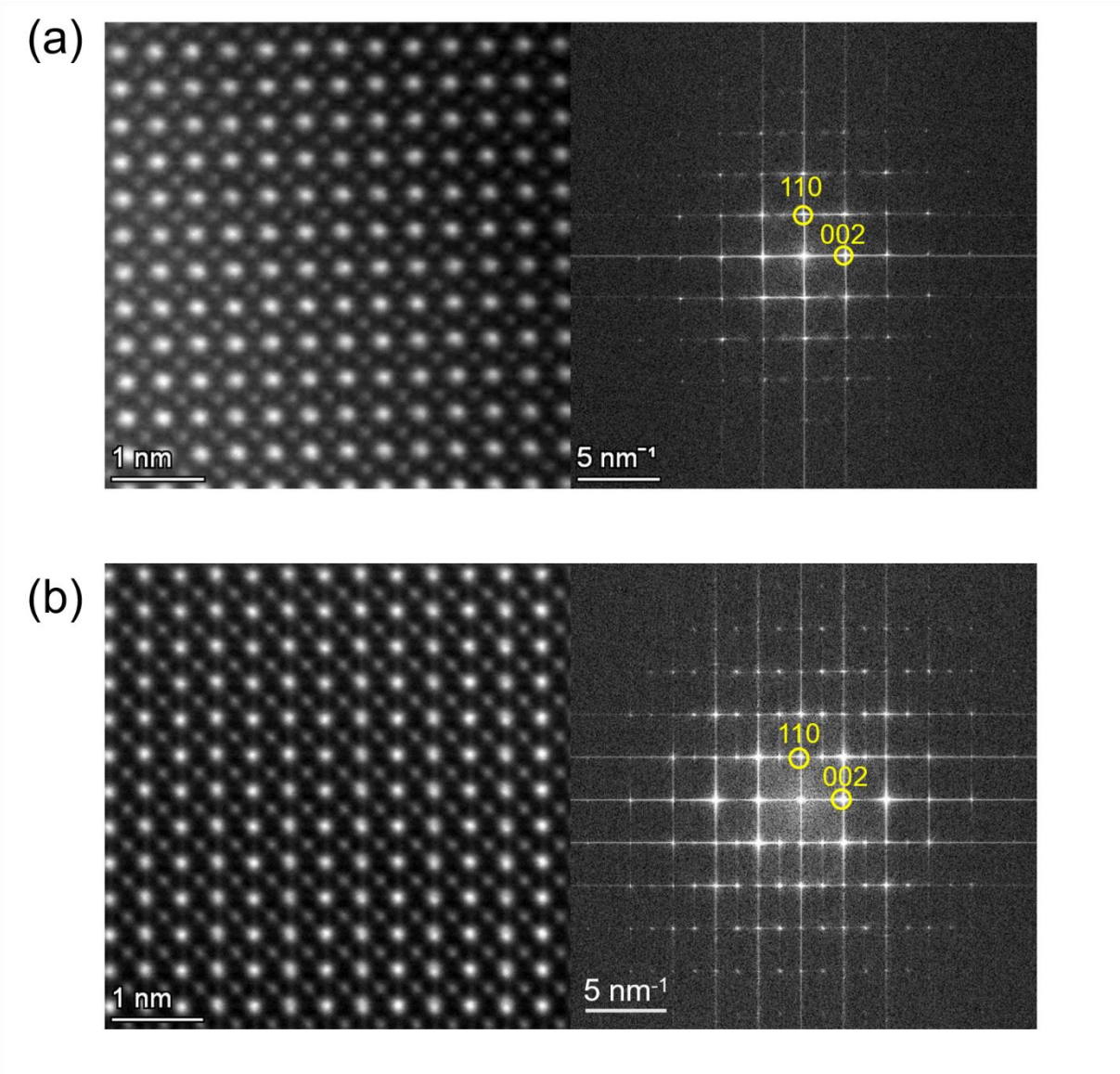

Figure S2. HAADF-STEM micrographs and corresponding FFTs from the [110] zone axis of x = 0.2 and 0.3 systems indicate the phase-pure *Pbnm* structure for both the systems.

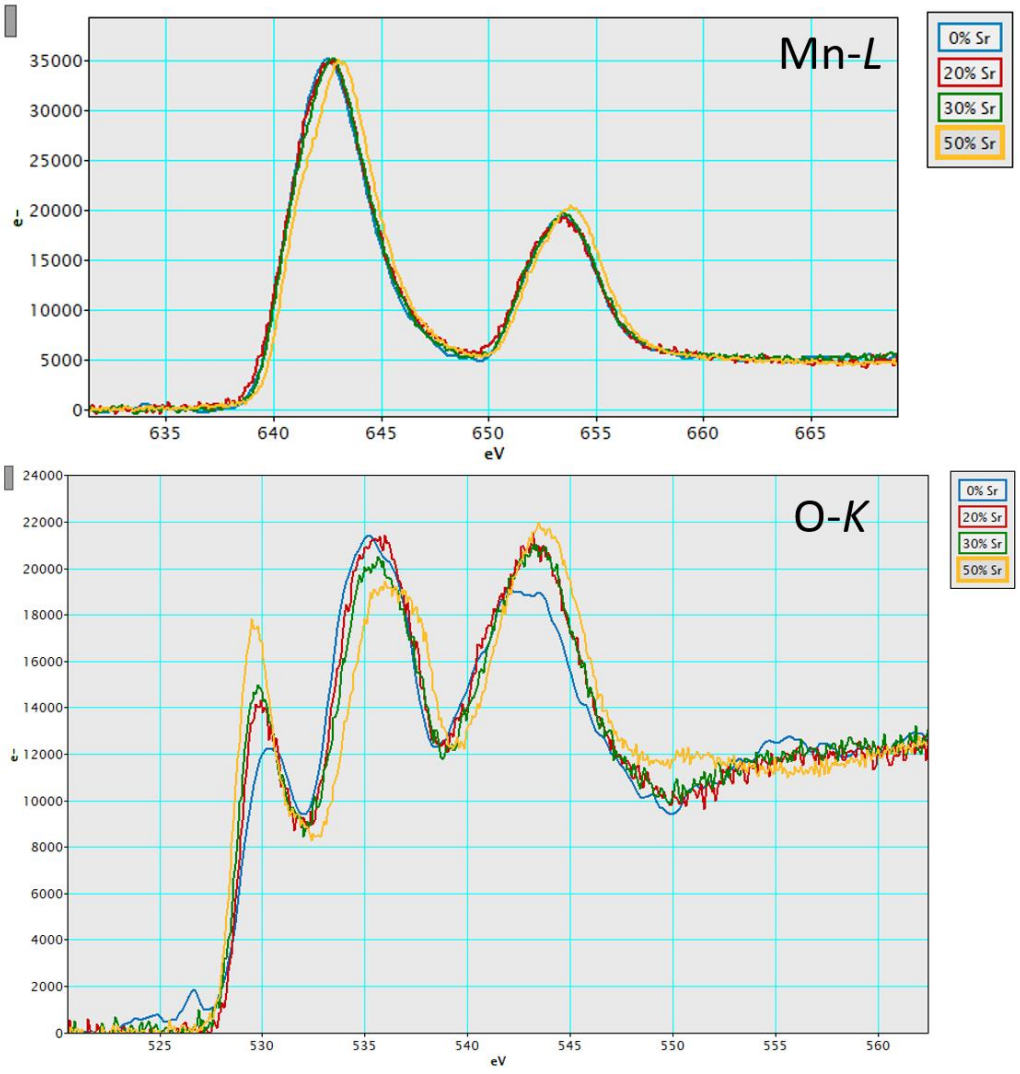

Figure S3. EELS spectra of the Mn-*L* and O-*K* edge for x = 0, 0.2, 0.3 and 0.5.

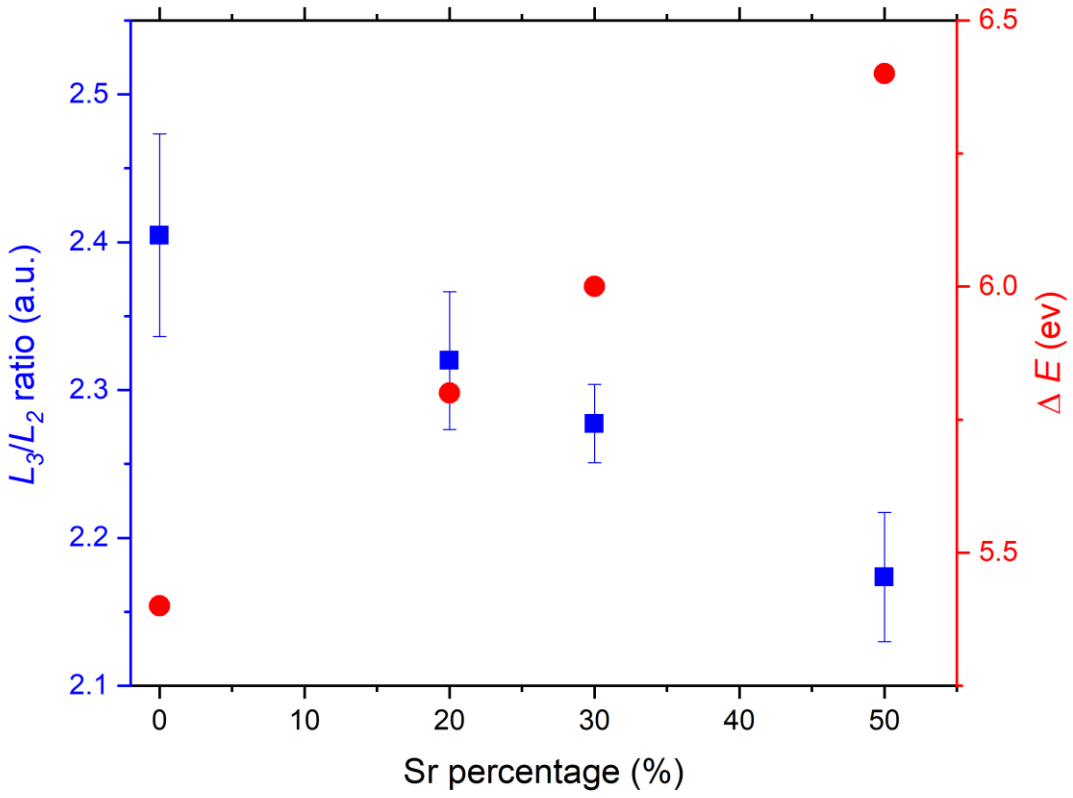

Figure S4. L_3/L_2 ratio and ΔE (as mentioned in the main manuscript) obtained from the EELS spectra for the samples with different amount of Sr doping. The decrease in the L_3/L_2 ratio and increase of the ΔE indicate an increase of the Mn^{4+}:Mn^{3+} ratio with increasing amount of Sr doping.

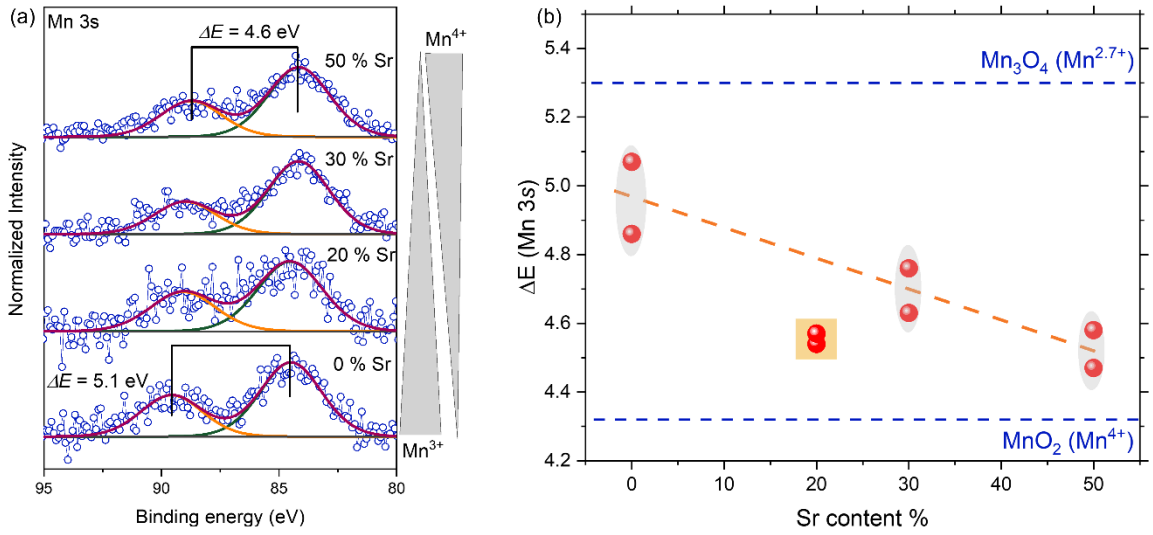

Figure S5. XPS analysis of the x = 0 (0 % Sr), 0.2 (20 % Sr), 0.3 (30 % Sr) and 0.5 (50 % Sr) and the two reference standards (MnO_2 and Mn_3O_4). a) Core-level Mn 3s XPS spectra (b) ΔE (splitting of Mn 3*s*) changes correspond to the changes in the oxidation state, where an increase in ΔE indicates a lower oxidation state of Mn. The estimation of the ΔE for the sample containing 20% Sr is quite unreliable due to the poor signal to noise ratio (very weak intensity).

The full spectrum from 0 eV to 1350 eV was measured for the x = 0, 0.2, 0.3 and 0.5 and two reference standards (MnO_2 and Mn_3O_4). For analysis, the core-level spectrum corresponding to Mn 3*s* was utilized, as the distinction between the oxidation states is more straightforward compared to the multiplet analysis of Mn 2p.[1] The peak separation observed in the splitting of Mn 3s spectrum (ΔE) strongly depends on the Mn oxidation state: a higher ΔE corresponds to a lower oxidation state of Mn.[2] Although a quantitative estimation of the oxidation state can be drawn based on the ΔE (Figure S5b), such a precise estimation has been avoided here as the ΔE show broad distribution for each sample. Nevertheless, the trend related to the change of the Mn oxidation state upon Sr doping is clear. Additionally, we would like to mention that for the 20 % Sr (x = 0.2) sample, the signal to noise ratio is poor for this sample (Figure S5a). Hence, the estimate of ΔE is not reliable for this system. Nevertheless, we have shown this data for completeness.

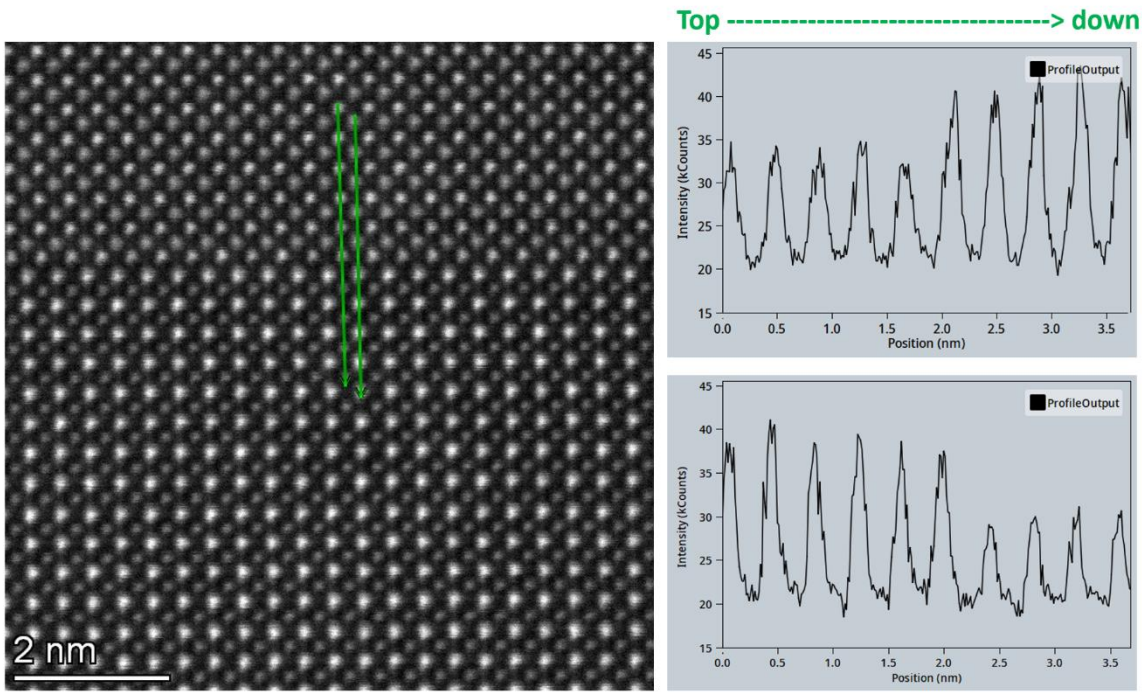

Figure S6. A stacking fault like lattice defect in x = 0.5.

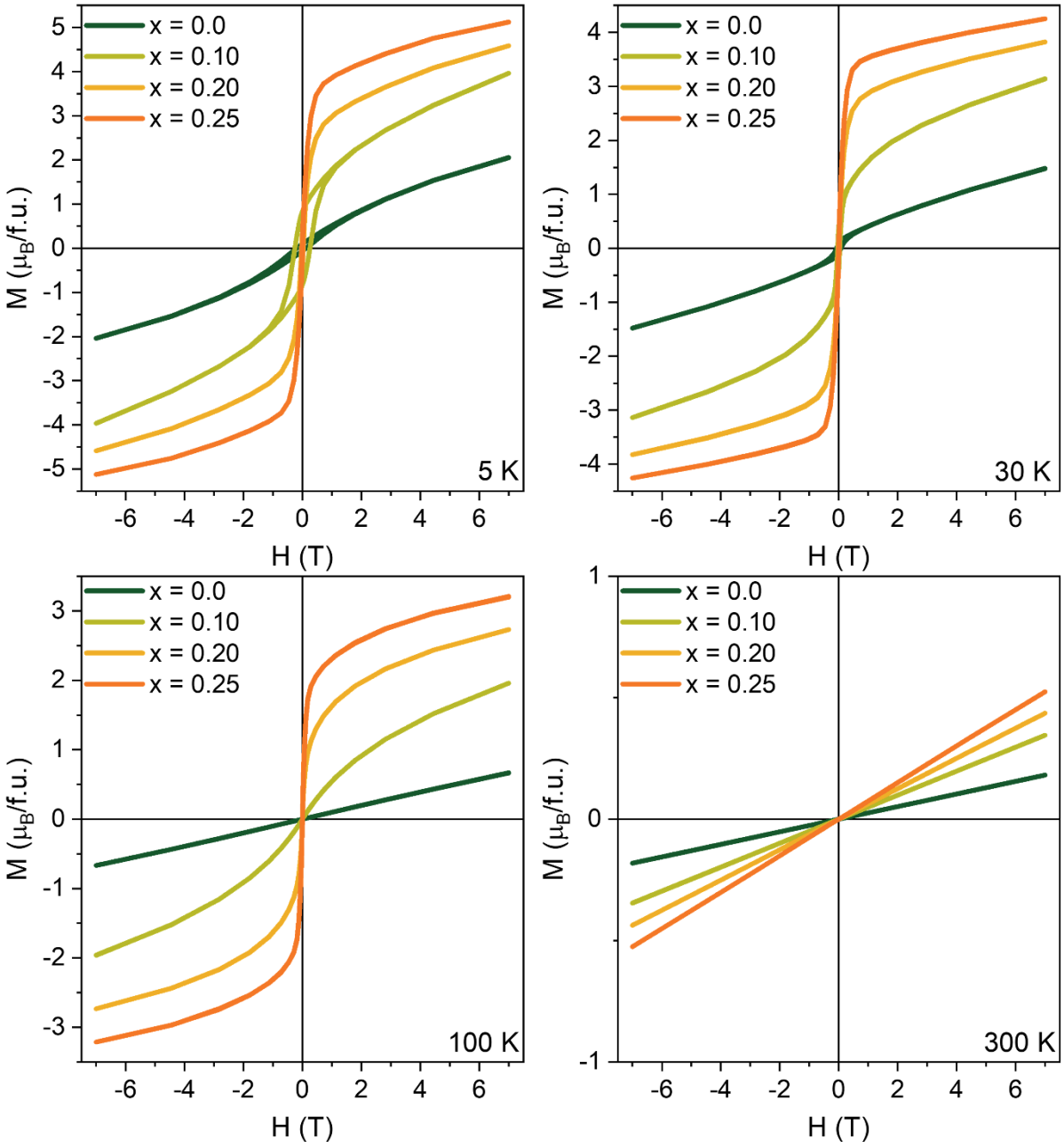

Figure S7. Magnetization of $(Gd_{0.25}La_{0.25}Nd_{0.25}Sm_{0.25})_{1-x}Sr_xMnO_3$ as a function of field at different temperatures, 5 K, 30 K, 100 K and 300 K.

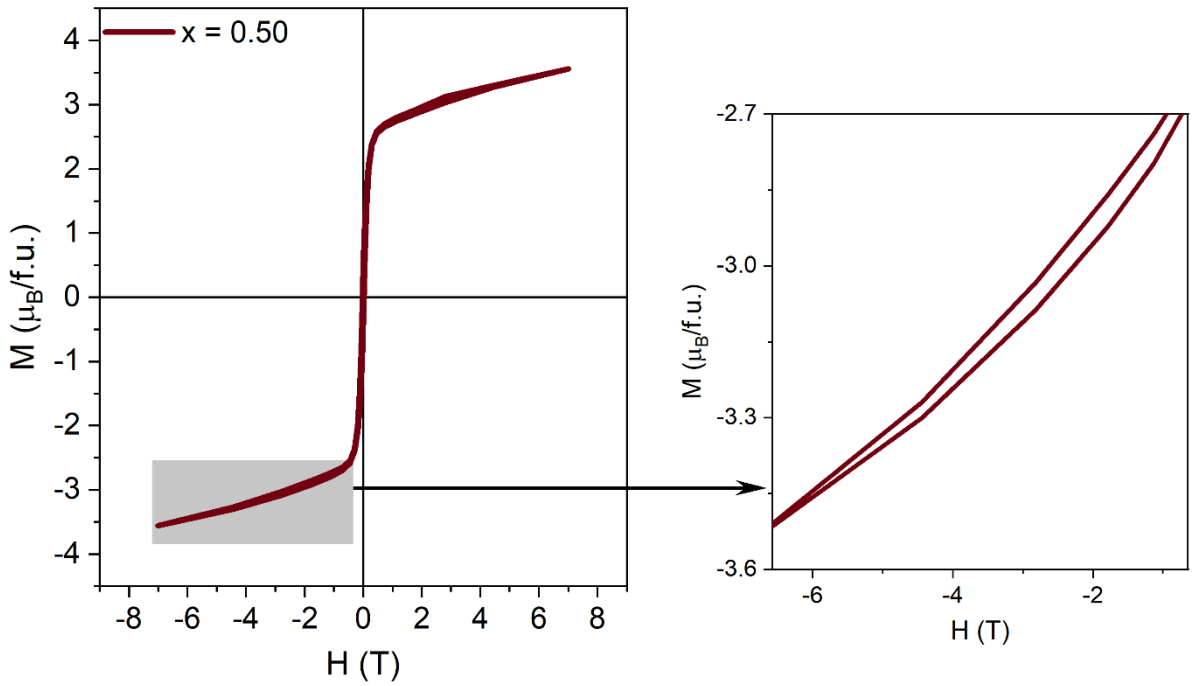

Figure S8. Magnetization of $(Gd_{0.25}La_{0.25}Nd_{0.25}Sm_{0.25})_{0.5}Sr_{0.5}MnO_3$ at 30 K, showing a presence of hysteresis even at higher external fields, which indicates magnetic phase separation (possibly consisting of a dominant soft FM part along with a hard FM or canted AFM part).

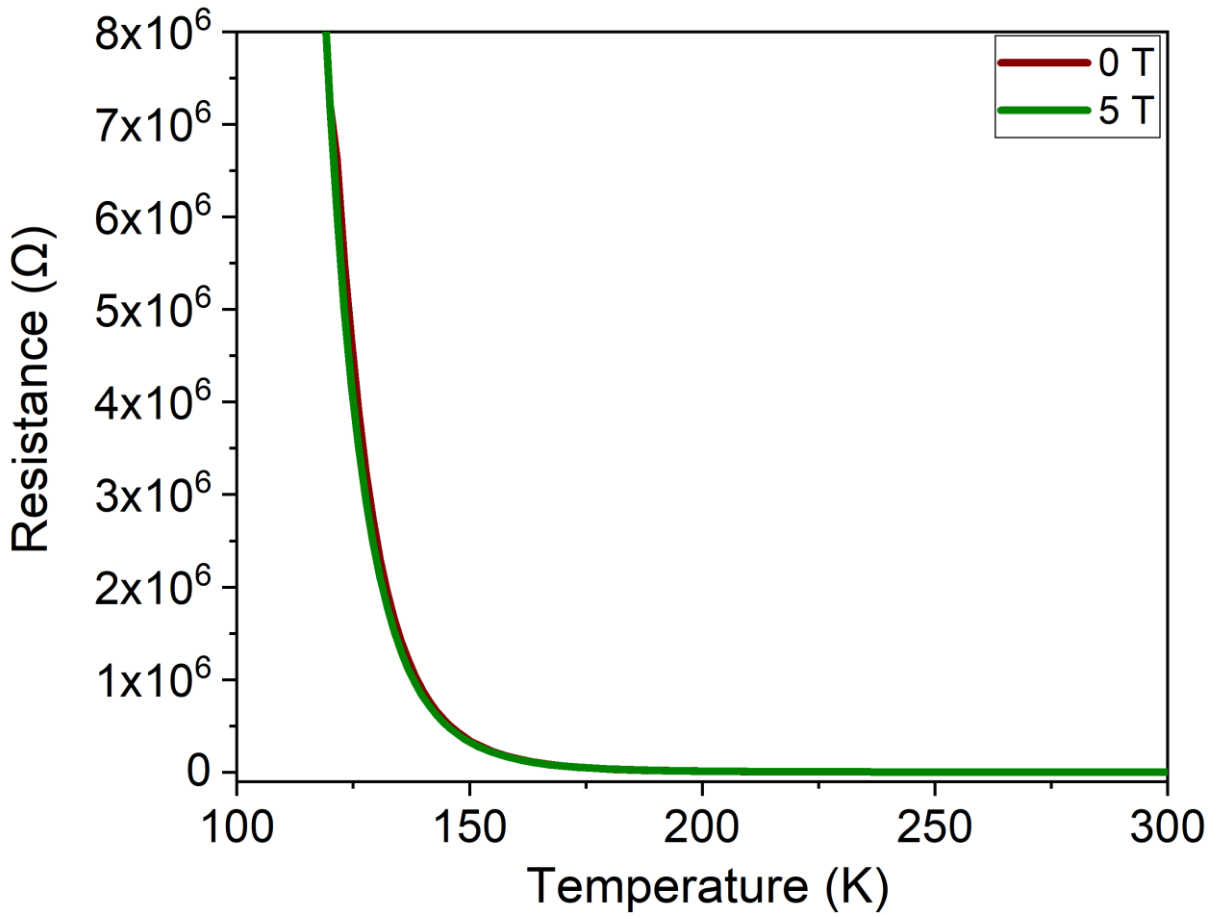

Figure S9. 4-probe resistance (Ω) as a function of temperature at two different external magnetic field (0 and 5 T) for $(Gd_{0.25}La_{0.25}Nd_{0.25}Sm_{0.25})_{0.9}Sr_{0.1}MnO_3$, indicating extremely high resistance values at lower temperatures, typical of an insulating material.

References

[1] R. Azmi, V. Trouillet, M. Strafela, S. Ulrich, H. Ehrenberg, M. Bruns, *Surf. Interface Anal.* **2018**, *50*, 43.

[2] Q.-H. Wu, M. Liu, W. Jaegermann, *Mater. Lett.* **2005**, *59*, 1980.